NREL
NATIONAL RENEWABLE ENERGY LABORATORY

Spectroradiometer Intercomparison and Impact on Characterizing Photovoltaic Device Performance

Preprint

A. Habte,[1] A. Andreas,[1] L. Ottoson,[1]
C. Gueymard,[2] G. Fedor,[3] S. Fowler,[3]
J. Peterson,[4] E. Naranen,[5] T. Kobashi,[6]
A. Akiyama,[6] and S. Takagi[6]

[1] *National Renewable Energy Laboratory*
[2] *Solar Consulting Services*
[3] *Q-Lab Corporation*
[4] *University of Oregon*
[5] *ATLAS Material Testing Technology, LLC*
[6] *EKO Instruments, Inc.*

Presented at Solar 2014
San Francisco, California
July 6–10, 2014

NREL is a national laboratory of the U.S. Department of Energy
Office of Energy Efficiency & Renewable Energy
Operated by the Alliance for Sustainable Energy, LLC

This report is available at no cost from the National Renewable Energy Laboratory (NREL) at www.nrel.gov/publications.

Conference Paper
NREL/CP-5D00-62215
November 2014

Contract No. DE-AC36-08GO28308

This report is available at no cost from the National Renewable Energy Laboratory (NREL) at www.nrel.gov/publications.

Available electronically at http://www.osti.gov/scitech

Available for a processing fee to U.S. Department of Energy and its contractors, in paper, from:

U.S. Department of Energy
Office of Scientific and Technical Information
P.O. Box 62
Oak Ridge, TN 37831-0062
phone: 865.576.8401
fax: 865.576.5728
email: mailto:reports@adonis.osti.gov

Available for sale to the public, in paper, from:

U.S. Department of Commerce
National Technical Information Service
5285 Port Royal Road
Springfield, VA 22161
phone: 800.553.6847
fax: 703.605.6900
email: orders@ntis.fedworld.gov
online ordering: http://www.ntis.gov/help/ordermethods.aspx

Cover Photos: (left to right) photo by Pat Corkery, NREL 16416, photo from SunEdison, NREL 17423, photo by Pat Corkery, NREL 16560, photo by Dennis Schroeder, NREL 17613, photo by Dean Armstrong, NREL 17436, photo by Pat Corkery, NREL 17721.

Spectroradiometer Intercomparison and Impact on Characterizing Photovoltaic Device Performance

Aron Habte,[1] Afshin Andreas,[1] Larry Ottoson,[1] Chris A. Gueymard,[2] Greg Fedor,[3] Sean Fowler,[3] Josh Peterson,[4] Erik Naranen,[5] Tsukasa Kobashi,[6] Akihito Akiyama,[6] and Shin Takagi[6]

1. National Renewable Energy Laboratory, 15013 Denver West Parkway, Golden, CO 80401
2. Solar Consulting Services, P.O. Box 392, Colebrook, NH 03576
3. Q-Lab Corporation, 800 Canterbury Road, Cleveland, OH 44145
4. University of Oregon, Department of Physics, 1274-Univ. of Oregon, Eugene, OR 97403-1274
5. ATLAS Material Testing Technology, LLC, 45601 N 47th Ave, Phoenix, AZ 85087
6. EKO instruments, Inc., 95 South Market Street, Suite 300, San Jose, CA 95113

ABSTRACT

Indoor and outdoor testing of photovoltaic (PV) device performance requires the use of solar simulators and natural solar radiation, respectively. This performance characterization requires accurate knowledge of spectral irradiance distribution that is incident on the devices. Spectroradiometers are used to measure the spectral distribution of solar simulators and solar radiation. On September 17, 2013, a global spectral irradiance intercomparison using spectroradiometers was organized by the Solar Radiation Research Laboratory (SRRL) at the National Renewable Energy Laboratory (NREL). Ten spectroradiometers from different laboratories participated in the intercomparison. The intercomparison aimed to understand the performance of the different spectroradiometers and to achieve internal performance-based measurement and calibration quality-control checks undertaken by the laboratories. The Simple Model of the Atmospheric Radiative Transfer of Sunshine (SMARTS) model outputs were used in the outdoor intercomparison as an explanatory tool. The intent was to better understand how well the SMARTS-modeled spectra compare to various types of spectroradiometers considering that the model has a finer resolution than the instruments under scrutiny. Aside from spectral regions corresponding to sharp absorption bands and fast-changing sky conditions, the overall results of the comparison demonstrated less than 10% difference among the participating spectroradiometers and between the measured and SMARTS outputs. The results of this first intercomparison will help to decrease systematic inter-laboratory differences in the measurements of the outputs or efficiencies of PV devices and harmonize laboratory experimental procedures.

Keywords: Spectral Irradiance; Spectroradiometer; Photovoltaic; PV; Simple Model of the Atmospheric Radiative Transfer of Sunshine; SMARTS

1. Introduction

On September 17, 2013, an indoor and outdoor spectral irradiance intercomparison using 10 spectroradiometers was organized by the National Renewable Energy Laboratory's (NREL's) Solar Radiation Research Laboratory (SRRL). In addition to NREL, EKO instruments, Inc.; Q-Lab Corporation; ATLAS Material Testing Technology, LLC; and the University of Oregon's Department of Physics participated in the intercomparison. A coordinated measurement setup and a common platform were employed to compare spectral irradiances under both indoor and outdoor conditions. The intercomparison was aimed at understanding the performance of the different spectroradiometers and sharing knowledge in making spectral irradiance measurements. Further, the characterization of solar simulators that are used to measure the energy output of photovoltaic (PV) modules depends on accurate spectral irradiance using spectroradiometers; therefore, understanding the performance of these different spectroradiometers will assist in better understanding the solar spectrum, which ultimately provides better energy output estimation of PV modules. Similar intercomparisons of spectroradiometers for solar applications have been conducted in other countries (see, for example, references (1) and (2)), and their results have been beneficial to improving laboratories' specialized spectral measurement capabilities, reducing metrological sources of errors, and increasing result comparability despite differing equipment. In the United States, interagency intercomparisons had been conducted only for ultraviolet spectroradiometers (3), (4), thus the present study was the first of its kind.

2. METHOD AND RESULT

To provide an unbiased assessment of the intercomparison, a mutually agreed-upon framework was developed. The framework included the following:

1. The process and analysis of the data from the individual laboratories is to be kept confidential. Each organization is identified in the report using only a generic name (Lab-1, Lab-2, NREL-1, NREL-2, etc.);
2. All participating spectroradiometers should have the same measurement setup, such as the outdoor measurement height and indoor measurement setup;
3. The start and end time of the outdoor measurement should be determined using the slowest scanning instrument; and
4. The comparison should be made using the common wavelength range from the participating spectroradiometers (380 nm to 1,100 nm).

The measurement was conducted indoors and outdoors using multiple spectroradiometers under controlled laboratory conditions and under clear-sky conditions around solar noon, respectively. Prior to the comparison, each instrument was calibrated either by the participant laboratory or by a recognized outside laboratory. In this report, no major effort was made to harmonize the inherent differences among instruments in terms of differing calibration date, instrument integration/measurement time, bandwidth size, or wavelength interval. The post processing of the indoor and outdoor comparisons was made at 5-nm intervals. Data from instruments with a higher resolution (less than 5 nm) were linearly interpolated to 5 nm before the indoor and outdoor data sets were compared. Further, all spectroradiometers sat on the same height of measurement to avoid any occlusion of one instrument by another from the entire sky vault (180°). This means that all spheres, cosine receptors, and diffusers sat 25 cm above the sitting surface. A run is determined by the duration of time that the slowest instrument takes to finish its scan. For the outdoor measurements, each instrument had a specific time interval within which to finish a measurement scan for the specified wavelength range. Therefore, instruments with faster time scans continued to measure until the slowest instrument finished its scan. Then, to obtain a comparable data set, the multiple files from the fast instruments were averaged to obtain one single result file with which the comparison analysis was performed for each run. All of the outdoor measurements were made within ±1.5 hour from solar noon, thus determining a period during which the sun's zenith angle was lower than 43.5 degrees.

The indoor comparisons were performed using NREL's FEL tungsten lamp (F407), which NREL does not use to calibrate spectroradiometers. This specific FEL lamp had less than 37 hours of usage and demonstrated good repeatability through time. The intent of the indoor comparison was to identify subtle shifts and trends that would be clearly seen in each spectroradiometer measurement due to factors such as differing calibration laboratories, methods of calibration setup, or type of lamp used to calibrate the instruments. Therefore, one spectroradiometer from each calibration laboratory was selected. During the indoor comparison, each instrument setup was the same, and data collection was made by the owner of each instrument. Simulations using the Simple Model of the Atmospheric Radiative Transfer of Sunshine (SMARTS) were applied to the outdoor intercomparison as an explanatory tool and to understand how well the SMARTS-modeled spectra compare to various types of spectroradiometers considering the model's spectral resolution compared to the spectroradiometers under scrutiny. Running the smoothing postprocessor of the SMARTS model was therefore necessary to downgrade the resolution of its spectra and make them match that of any specific instrument based on the shape of its passband (e.g., Gaussian), its width (as measured by the full width at half maximum), and its wavelength step (e.g., 5 nm).

TABLE 1. PARTICIPATING SPECTRORADIOMETER CHARACTERISTICS

Organization	Type of Spectroradiometer	Wavelength Range (nm)	Entrance Optics	Calibration Standard/Lamp	Detector	Calibrating Laboratory and Date of Calibration
NREL (SRRL)	OL750	280–2,400	Integrating sphere (6-inch)	NIST FEL Lamp F655 ASTM G138	Silicon/Ge/Pbs	NREL Optical Metrology Laboratory September 16, 2013
EKO Instruments, Inc.	WISER: MS-710/ MS-712 (Polychromator)	350–1,700	Dome/ diffuser	Optronics FEL Lamp ASTM G138	MS710: Silicon diode array/MS712: InGaAs diode array	Optronics December 20, 2012
NREL (SRRL)	LI-1800	380–1,100	Cosine receptor	NIST FEL Lamp F655 ASTM G138	Silicon	NREL Optical Metrology Laboratory April 15, 2013
Q-Lab Corporation	OL750/ Double Monochromator	280–1,100	Integrating sphere (6-inch)	Optronics FEL Lamp ASTM G138	Silicon	Gooch & Housego, traceable to NIST May 20, 2013
NREL (Device Performance Group)	ASD	350–2,400	Integrating sphere (4-inch, with dome)	NIST FEL Lamp F655 ASTM G138	Silicon diode array/InGaAs high-speed rotating grating/Extended infrared InGaAs high-speed rotating grating	NREL Optical Metrology Laboratory June 11, 2013
NREL (Device Performance Group)	LI-1800 (with NREL temperature controller)	380–1,100	Cosine receptor	NIST FEL Lamp F655 ASTM G138	Silicon	NREL Optical Metrology Laboratory June 13, 2013
NREL (SRRL)	Pulse Analysis Spectroradiometer System (PASS)	280–1,720	Integrating sphere (6-inch)	NIST FEL Lamp F655 ASTM G138	Silicon/InGaAs	NREL Optical Metrology Laboratory September 16, 2013
ATLAS	OL770 CCD Array	380–1,100	Integrating sphere (2-inch)	OL752-10 Plug-in Standard ASTM G138	Silicon diode array	ATLAS September 4, 2013
University of Oregon	LI-1800 (with University of Oregon temperature controller)	380–1,100	Cosine receptor	LICOR 1800-02 Optical Radiation Calibrator (ORC) ASTM G138	Silicon	LICOR, traceable to NIST September 29, 2011

Instrument information including entrance optics, wavelength range, detector type, and calibration date is described in Table 1.

The NREL-1 system was considered a reference instrument for the indoor comparison because it is reliable, repeatable, and has less uncertainty than the other NREL spectroradiometers that participated in this intercomparison. The indoor comparison results shown in Fig. 1 demonstrate the performance of each participating spectroradiometer relative to the NREL-1 system.

The ratios in Fig. 1 show differences from one instrument to another. Lab-3 showed the closest similarity relative to the NREL-1 spectroradiometer, and Lab-4 showed higher differences. Another observation from the indoor comparison was that Lab-1 values were persistently lower (average 1.3%) than the NREL-1 instrument, whereas Lab-2 values were persistently higher, by approximately 3.6% on average. Lab-4 was higher below the 750-nm and higher above the 750-nm mark. These differences could have resulted from multiple reasons, including differences in calibration procedures, differing calibration setups from one laboratory to another, differing environmental conditions inside laboratories, whether a primary or secondary spectral irradiance calibration lamp was used for the calibrations, instrument age, and time elapsed since the last calibration. Further, the differences could be related to the instrument design, such as spectral resolution (based on quoted specification or slit widths). For example, WISER specification for spectral resolution is 5 nm, but OL 750 resolution depends on the width of the selected input and output slits (which are changeable), and ASD specification depends on the internal configuration of the ASDs. These variations may significantly contribute to the differences observed among radiometers.

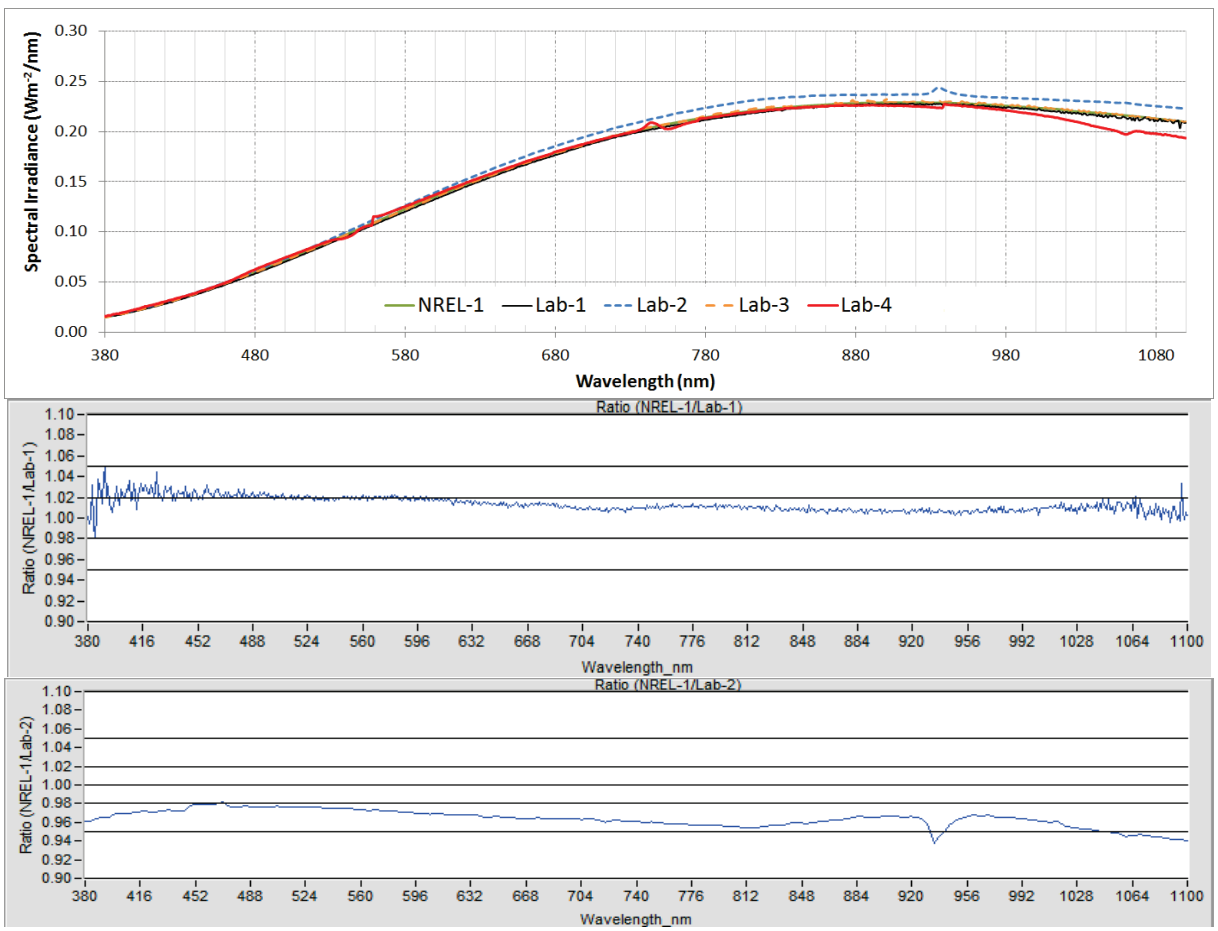

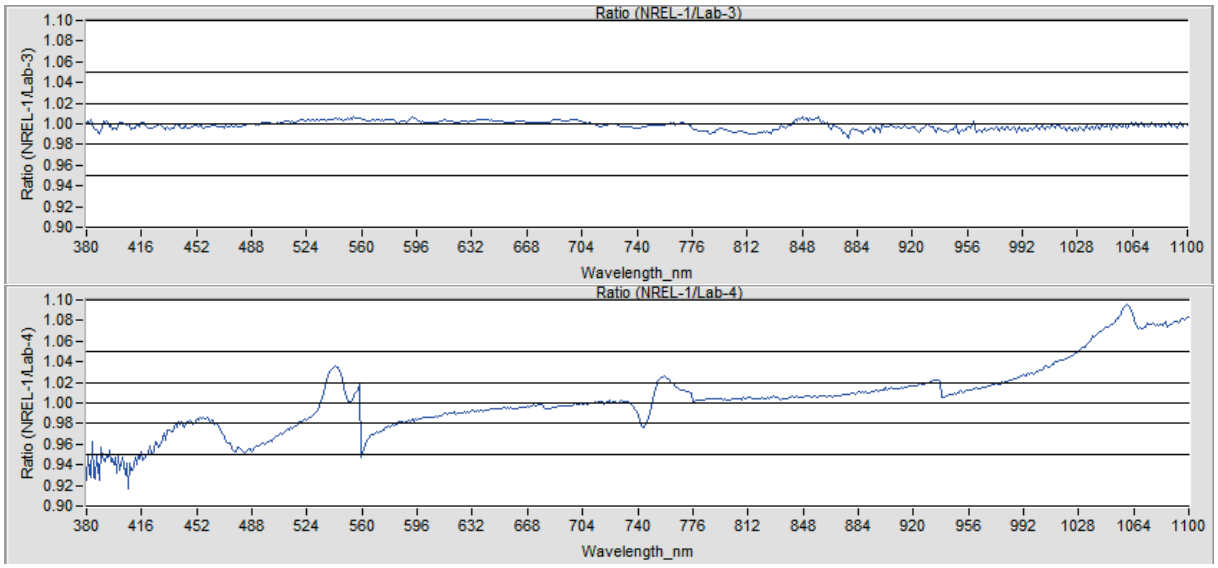

Fig. 1. Plots showing indoor differences and ratios performed using the NIST FEL lamp. The top plot shows the spectral irradiance in Wm-2 nm-1 versus wavelength (nm). The bottom four plots show the spectral irradiance ratios relative to the NREL-1 instrument.

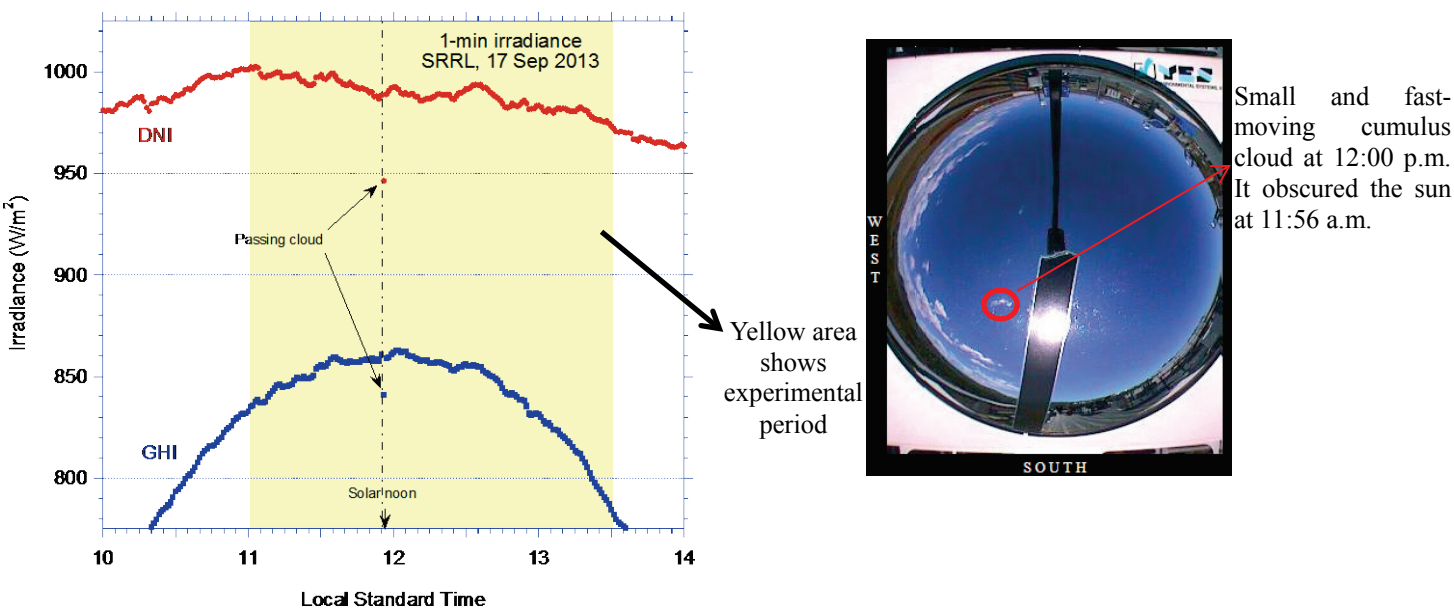

Fig 2. (Left) One-minute broadband data for global horizontal irradiance and direct normal irradiance during the experimental period showing the rapid variations in both signals, the decreasing trend in direct normal irradiance after 11:00 LST, and the impact of the passing cumulus cloud at solar noon. (Right) Image from the TSI-880 (Sky Imager) showing the passing of the small cumulus cloud.

The outdoor comparison was performed around solar noon. The selection of the solar noon period has significant advantages because there is a reduction in inadvertent sources of errors and irradiance variations are limited during the measurements, especially when slow-scanning instruments are used. During the outdoor event, clear-sky conditions prevailed, except for a very short period (a few seconds) at solar noon during which a small and fast-moving cumulus cloud obscured the sun. The broadband irradiance measurement accompanied with the sky imager data show this slight and rapid irradiance perturbation (Fig. 2). Two of the NREL spectroradiometers collected data at 5-nm intervals. Therefore, to obtain comparable results, the outdoor data analysis was performed at 5-nm intervals for all instruments for a common wavelength range (380 nm to 1,100 nm). A linear interpolation method was applied to data sets obtained from the instruments that have a higher resolution. Further, the time used for each measurement run was determined by the time taken by the slowest instrument to finish its scan, i.e., approximately 45 minutes. The data from the faster instruments was averaged to perform the analysis.

The measured data from each spectroradiometer and the modeled data from the SMARTS model were divided by the average values calculated from all measured data. Aside from spectral regions corresponding to sharp absorption bands, a fast-moving cloud (Fig. 2), or spikes detected in one instrument due to unknown conditions, the relative difference among the instruments was less than 10% (Fig. 3 (right)).

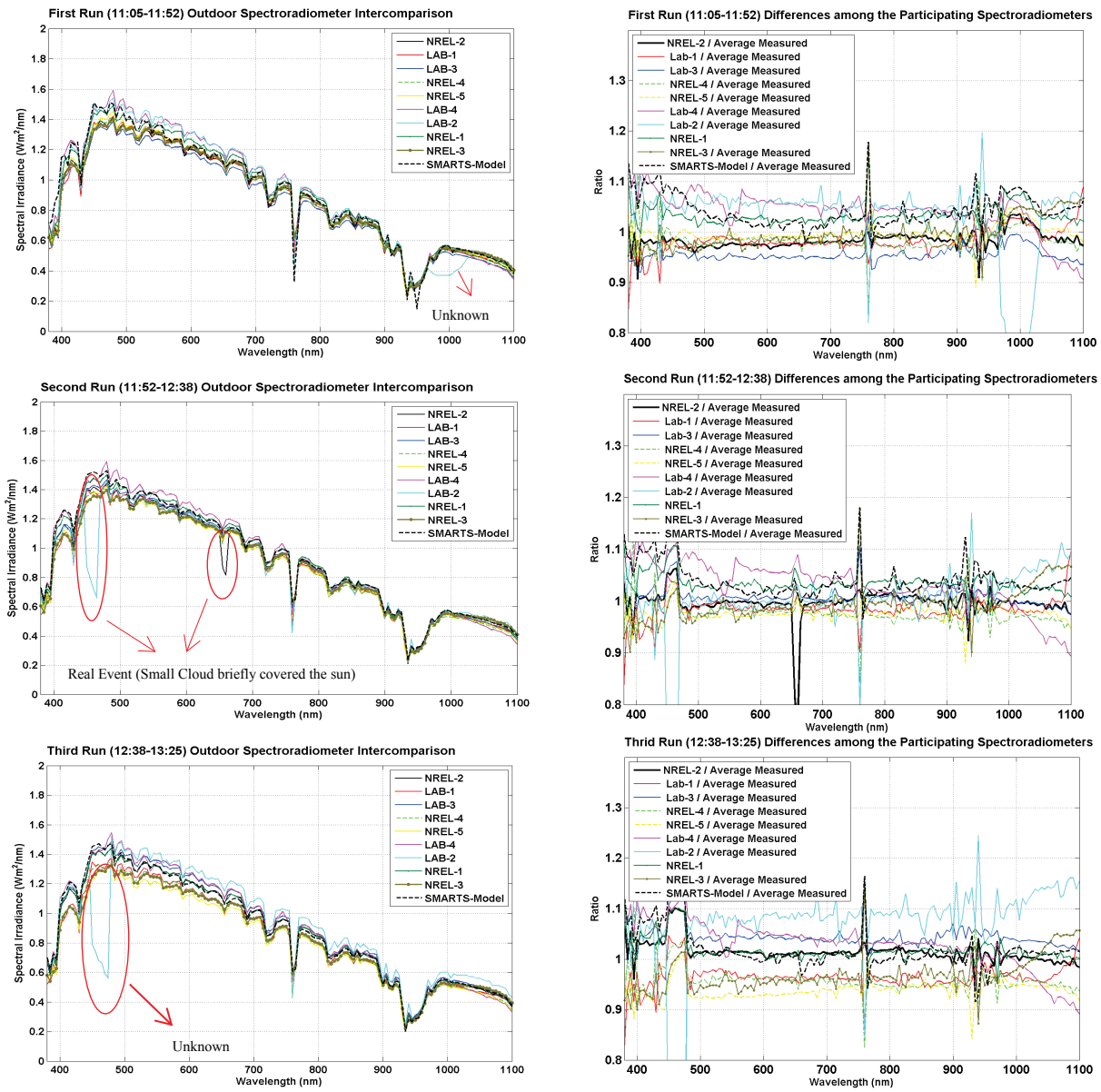

Fig. 3. The three outdoor runs, from top to bottom, showing the (left) spectral irradiance plot for each participating spectroradiometer and SMARTS model spectral irradiance output and (right) ratio using the average spectrum from the participating spectroradiometers.

Solar noon on September 17, 2013, occurred at approximately 11:54:30 LST, coinciding almost exactly with the passage of the noted small cumulus cloud (Fig. 2 and 3). Except for such anomalous conditions, runs conducted close to solar noon are expected to yield lower differences in results than at any other time of the day. Indeed, the second run period, which was very close to solar noon, demonstrated relatively smaller differences. The second run had comparatively less air mass because of the smallest solar zenith angles of the day. The second run also had less variation in global horizontal irradiance during scan times.

The 380-nm to 400-nm and 1,000-nm to 1,100-nm spectral bands showed relatively higher differences compared to the rest of the spectrum. The relative higher percent difference of the former band could be related to the lower performance of most spectroradiometers in the ultraviolet region coupled with the

higher uncertainty in the output of the calibration lamps (5). The latter range (in the near infrared) could be related to the temperature dependence of the silicon detectors. In particular, out of the three LICOR 1800s, one was not equipped with a temperature controller during the intercomparison. Moreover, one of the temperature-controlled LICOR 1800s may have been calibrated at a different temperature than what was used during the intercomparison. In any case, the larger uncertainty of that instrument below 400 nm and above 900 nm has previously been described in the literature (6), (7).

We also attempted to show any presence of systematic (bias) or random (scatter) tendencies in the spectral irradiance measurement from each spectroradiometer relative to the measured spectral irradiance averaged throughout 100-nm wide spectral bands and among all instruments. To perform these calculations, mean bias error (MBE) and root mean square error (RMSE) were calculated. The results are shown in percent MBE and RMSE, and they are relative to the average reading of the hundred-wavelength bins. Further, the MBE and RMSE were averaged for the three outdoor runs, as shown in Table 2. Lab-1 had a larger negative MBE for the 380-nm to 400-nm bin. Lab-4 had a larger positive MBE, between 380 nm and 500 nm. Lab-2 appeared to have a higher RMSE for the 400-nm to 500-nm range. As described previously, this is likely related to the fast-moving cloud that obscured the sun during the second run and to the unknown experimental condition that occurred during the third outdoor run. Another unknown condition is responsible for the poor performance of Lab-2 in the 900-nm to 1,100-nm range. However, it is important to note that the differences shown in Table 2 are average differences from the three outdoor runs and result from the aggregation of hundred-wavelength bins. Because of this averaging of multiple runs and to the spectral aggregation method, relatively low differences were likely obtained because of error cancellations. Overall, the minimum and maximum MBE of the average of all bins for all spectroradiometers are -3% and 3.9%, respectively, and for RMSE, they are between 2.5% and 8.5%, respectively. The results of the root sum of the squares (RSS) for both the minimum and maximum of the MBE and RMSE are between approximately 4% and 10%. The RSS values are typical for such comparisons (8).

As illustrated in the above results, in parallel to the outdoor intercomparison, a SMARTS model experiment was conducted to understand additional information that may be offered by using the modeled spectra. This avenue provided relevant information in previous similar intercomparisons (1), (2). As in these earlier studies, the SMARTS code (9), (10) was retrospectively used to obtain modeled spectra at the time of the measurements. The model has a finer resolution than the instruments under scrutiny. Running the smoothing postprocessor of SMARTS was therefore necessary to downgrade the resolution of its spectra and make it match that of any specific instrument based on the shape of its passband (e.g., Gaussian), its width (as measured by the full width at half maximum), and its wavelength step (e.g., 5 nm). Simulations of global spectral irradiance using SMARTS are shown in Fig. 8 for an assumed instrument with a Gaussian 5-nm bandpass and 1-nm wavelength step. These spectra correspond to the mid-times of the three individual runs (11:30 LST, 12:15 LST, and 13:00 LST), yielding air masses of 1.27, 1.27, and 1.32, respectively. Additional locally measured meteorological input parameters were supplied to the SMARTS model. These are station pressure (nearly constant): approximately 816 mb; total ozone amount (average for that day): 0.281 atm-cm; total nitrogen dioxide amount (default value): 0.2 matm-cm; precipitable water (measured by SRRL's global positioning system): 1.20 cm to 1.41 cm; aerosol optical depth at 500 nm (average of measured value from two sunphotometers at SRRL): 0.06; Ångström exponent (derived from the direct spectrum measured with a PGS100 instrument located at SRRL): 2.0; aerosol single-scattering albedo (derived from sunphotometer data using an inversion method from SRRL): 0.98; aerosol asymmetry factor (derived from sunphotometer data using an inversion method from SRRL): 0.71; and spectral surface reflectance (assumed; selected from the SMARTS library): dry grass.

TABLE 2. AVERAGE MBE AND RMSE IN PERCENT

Bins	Average of All vs. NREL-1		Average of All vs. NREL-2		Average of All vs. NREL-3		Average of All vs. NREL-4		Average of All vs. NREL-5		Average of All vs. Lab-1		Average of All vs. Lab-2		Average of All vs. Lab-3		Average of All vs. Lab-4	
	MBE (%)	RMSE (%)	MBE (%)	RMSE (%)	MBE (%)	RMSE (%)	MBE (%)	RMSE (%)	MBE (%)	RMSE (%)	MBE (%)	RMSE (%)	MBE (%)	RMSE (%)	MBE (%)	RMSE (%)	MBE (%)	RMSE (%)
380–400	4.83	6.06	-0.75	4.85	-5.98	6.31	0.02	7.85	-3.06	5.37	-8.18	9.77	6.1	7.11	-1.18	3.76	8.18	8.44
400–500	4.88	5.55	1.2	3.6	-3.72	4.49	-1.9	3.88	-2.92	3.77	-2.68	4.57	-4.85	17.52	1.34	5.27	8.65	8.97
500–600	2.24	2.29	-0.57	1.52	-3.12	3.3	-2.47	2.54	-3.79	3.81	-1.92	2.04	4.24	4.94	-0.05	3.34	5.45	5.81
600–700	1.9	2.05	-1.43	3.52	-2.16	2.35	-2.57	2.69	-3.32	3.41	-2.42	2.51	4.94	5.42	-0.05	3.4	5.11	5.17
700–800	2.97	4.26	0.14	1.42	-0.77	4.35	-3.76	4.85	-2.79	3.27	-2.92	3.41	3.16	6.87	0.13	4.25	3.83	4.01
800–900	2.79	2.88	0.23	1.18	-1.28	1.85	-3.9	3.92	-2.73	2.96	-3.02	3.15	4.76	5.27	0.1	3.29	3.05	3.11
900–1,000	2.96	3.6	-0.31	2.6	-1.05	3.73	-2.64	4.76	-2.56	4.42	-1.61	2.44	2.35	10.19	1.1	3.52	1.77	2.78
1,000–1,100	2.25	2.53	-0.41	1.13	3.82	4.45	-3.06	3.46	-2.31	3.34	-0.96	2.55	5.84	11.04	-0.63	2.88	-4.55	5.83

Previously, an average of the measured spectral irradiance data was used to determine the differences among spectroradiometers. However, to avoid any bias that might be incurred by using instruments with no temperature controller or instruments with calibration problems that could eventually affect the averaging of the measured data, in this comparison one NREL instrument (NREL-2) was selected as a reference instrument for the outdoor comparison to understand the spectral irradiance differences between the spectroradiometers and SMARTS-modeled spectra. This does not mean that the NREL-2 is the best instrument among the participating spectroradiometers for outdoor measurements. Fig. 4 shows the ratio obtained by comparing each measured spectral data from the spectroradiometers and the SMARTS model spectral irradiance output to the NREL-2 spectral irradiance data set. Overall, the results showed differences within the ±10% limit. Note, however, that the ultraviolet and infrared regions edged close to this limit.

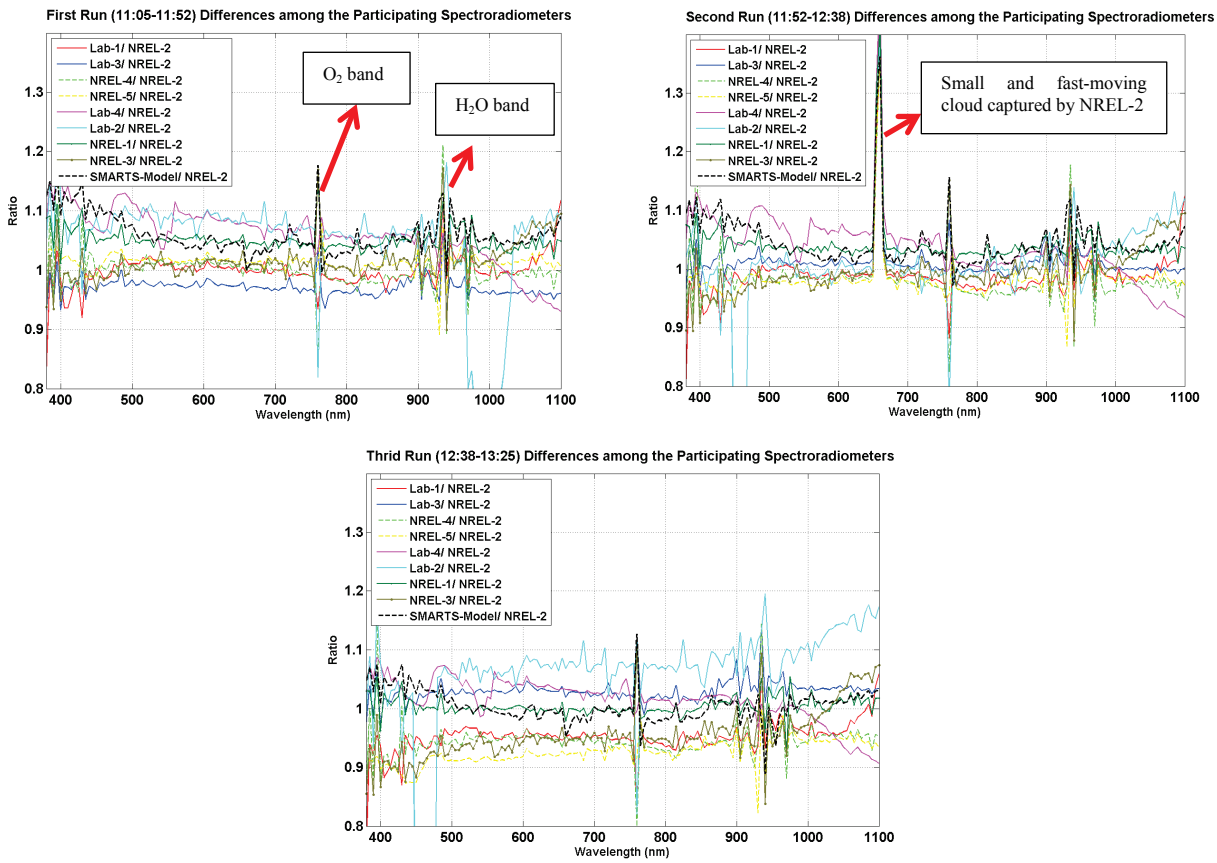

Fig. 4. Spectral irradiance data differences for the three runs

3. SUMMARY

Achieving higher penetrations of photovoltaic (PV) on the grid and reducing integration costs requires accurate knowledge of available the solar resource. One of the critical aspects of this is to understand the spectral irradiance characteristics of the incoming solar radiation. Spectroradiometers are often used to characterize solar spectral irradiance; therefore, understanding the characteristics of multiple spectroradiometers is essential to understanding the performance of PV systems.

The results from the intercomparison exercise described here provide various benefits, such as a better understanding of the performance of the different spectroradiometers under scrutiny. During the event, there were issues related to instrument functions and a few problems related to calibration issues. For instance, the calibration file did not work properly with the selected setting. Some of the problems were solved, and some were not. These types of issues, coupled with the inherent differences in instrument design such as spectral resolution (based on quoted specification or slit widths), calibration methods, and age; source of spectral irradiance calibration lamps; the amount of time since the last calibration of the instrument; incidence angle; reported calibration uncertainty by the laboratories; wavelength shift; environmental conditions; interpolation of data during the analysis; or other experimental issues are the primary reasons for the differences in spectral irradiance measurements in the analysis. The instruments that participated in the indoor tests demonstrated satisfactory comparisons. The outdoor comparison differences were within

±10%, but the ultraviolet and near-infrared spectral bands showed relatively higher differences than the rest of the spectrum. This is explained in part by the usually low performance of most spectroradiometers in the ultraviolet region (a known issue)—unless they are specifically designed to sense ultraviolet wavelengths. Moreover, the spectral irradiance calibration lamps, whether they are NIST primary FEL lamps or secondary lamps, have relatively higher uncertainty in the ultraviolet region due to their low output. Silicon detectors that are not stabilized using temperature controllers usually have low performance in the near-infrared region. This was indeed observed for some of them during the intercomparison. Overall, the RSS of the minimum and maximum of the MBE and RMSE averages are between approximately 4% and 10%, respectively, which is typical for these types of intercomparisons. Further, including simulated spectra from the SMARTS model in the outdoor intercomparison provides relevant information when predicting clear-sky solar spectral irradiance under varying atmospheric conditions. The output from the model compares well to the outdoor spectroradiometers' spectral irradiance output, and the differences were within the margin of error.

4. ACKNOWLEDGMENT

This work was supported by the U.S. Department of Energy under Contract No. DE-AC36-08-GO28308 with the National Renewable Energy Laboratory.

5. REFERENCES

(1) J.A. Martinez-Lozano, M.P. Utrillas, R. Pedros, F. Tena, J.P. Diaz, F.J. Exposito, J. Lorente, X. De Cabo, V. Cachorro, R. Vergaz, and V. Carreno, Intercomparison of Spectroradiometers for Global and Direct Solar Irradiance in the Visible Range, Journal of Atmospheric and Oceanic Technology (20), 2003; pp. 997–1,010.

(2) R. Galleano, W. Zaaiman, A. Virtuani, D. Pavanello, P. Morabito, A. Minuto, A. Spena, S. Bartocci, R. Fucci, G. Leanza, D. Fasanaro, and M. Catena, Intercomparison Campaign of Spectroradiometers for a Correct Estimation of Solar Spectral Irradiance: Results and Potential Impact on Photovoltaic Devices Calibration, Progress in Photovoltaics: Research and Applications, 2013. Accessed February 2014: http://onlinelibrary.wiley.com/doi/10.1002/pip.2361/full.

(3) K. Lantz, P. Disterhoft, E. Early, A. Thompson, J. DeLuisi, P. Kiedron, L. Harrison, J. Berndt, W. Mou, T.J. Erhamjian, L. Cabausua, J. Robertson, D. Hayes, J. Slusser, D. Bigelow, G. Janson, A. Beaubian, and M. Beaubian, The 1997 North American Interagency Intercomparison of Ultraviolet Monitoring Spectroradiometers, Journal of Research of NIST (National Institute of Standards and Technology) (107), 2002; pp. 19–62.

(4) A. Thompson, E.A. Early, J.J. DeLuisi, P. Disterhoft, D. Wardle, J. Kerr, J. Rives, Y. Sun, T. Lucas, T. Mestechkina, and P. Neale, The 1994 North American Interagency Intercomparison of Ultraviolet Monitoring Spectroradiometers, Journal of Research of NIST (National Institute of Standards and Technology) (102), 1997; pp. 279–322.

(5) H.W. Yoon and C. Gibson, NIST Special Publication 250-89—NIST Measurement Services: Spectral Irradiance Calibration, Gaithersburg, MD: National Institute of Standards and Technology, 2001. Accessed February 2014: http://www.nist.gov/calibrations/upload/sp250-89.pdf.

(6) V.E. Cachorro, A. Berjon, C. Toledano, S. Mogo, A.M. De Frutos, J.M. Vilaplana, M. Sorribas, B.A. De La Morena, J. Gröbner, and N. Laulainen, Detailed Aerosol Optical Depth Intercomparison between Brewer and Li-Cor 1800 Spectroradiometers and a Cimel Sun Photometer, Journal of Atmospheric and Oceanic Technology (26), 2009; pp. 1,558–1,573.

(7) D.R. Myers, Estimates of Uncertainty for Measured Spectra in the SERI Spectral Solar Radiation Data Base, Solar Energy (43), 1989; pp. 347–353.

(8) Walker, J. H., R. D. Saunders, J. K. Jackson, K. D. Mielentz, Results of a CCPR intercomparison of spectral irradiance measurements by national laboratories, J. Res. Natl. Inst. Stand. Technol., 96, 647–668, 1991.

(9) C.A. Gueymard, SMARTS2: A Simple Model of the Atmospheric Radiative Transfer of Sunshine: Algorithms and Performance Assessment, FSEC-PF-270-95, Cocoa, Florida: Florida Solar Energy Center, 1995. Accessed February 2014: http://www.solarconsultingservices.com/SMARTS2_report.pdf.

(10) C.A. Gueymard, Parameterized Transmittance Model for Direct Beam and Circumsolar Spectral Irradiance, Solar Energy (71), 2001; pp. 325–346.